Dissociation Energy of the Hydrogen Molecule

A. Balakrishnan, V. Smith,[a] and B. P. Stoicheff

Department of Physics, University of Toronto, and Ontario Laser and Lightwave Research Centre, Toronto, Ontario, Canada M5S 1A7

(Received 11 December 1991)

Fluorescence-excitation spectroscopy near 84.5 nm has been used to measure the threshold for the dissociation limit of $H_2(B'\,{}^1\Sigma_u^+) = H(1s) + H(2s)$ at $118\,377.06 \pm 0.04$ cm^{-1}. This yields a value of $D_0(H_2) = 36\,118.11 \pm 0.08$ cm^{-1} for the dissociation energy of the ground electronic state $X({}^1\Sigma_g^+)$ of H_2, in agreement with the latest theoretical calculation which includes nonadiabatic, relativistic, and radiative corrections. When combined with recent determinations of the ionization energy of H_2, the present $D_0(H_2)$ leads to the value $D_0(H_2^+) = 21\,379.36 \pm 0.08$ cm^{-1}, also in good agreement with theoretical values.

PACS numbers: 35.20.Gs, 33.20.Ni, 33.80.Gj

The precise experimental determination of the dissociation energy for the ground electronic state of the hydrogen molecule has long remained a challenge as a test of basic theory for this simplest of diatomic molecules. The latest calculation by Kolos, Szalewicz, and Monkhorst [1], based on 249-term wave functions and including relativistic, radiative, and nonadiabatic corrections, has yielded the value $D_0(H_2) = 36\,118.088$ cm^{-1}, with an estimated accuracy [2] of ± 0.10 cm^{-1}. The corrections themselves are small, and range from 0.2 to 0.5 cm^{-1}; consequently, experimental precision better than 0.2 cm^{-1} is required to confidently test the theory in all of its aspects. To date, however, experimental measurements have not achieved this level of accuracy.

In all previous experiments, the ground-state dissociation energy $D_0(H_2)$ has been derived from a measurement of the second dissociation limit of molecular hydrogen (Fig. 1) which converges to the atomic states $H(1s) + H(2s,2p)$. In 1970, Herzberg [3] investigated the absorption spectra of H_2, D_2, and HD at 77 K with a 10.5-m vacuum grating spectrograph. In spite of overlapping molecular lines in the region of the second dissociation limit, he obtained upper and lower bounds for the limit of H_2, and favored the upper bound at $118\,377.6$ cm^{-1}. This yielded a value of $D_0(H_2) = 36\,118.3$ cm^{-1}. At that time, Stwalley [4] made new vibrational assignments of the molecular lines near the limit, and by extrapolation, based on the long-range behavior of the internuclear potential, obtained a value of $118\,377.7 \pm 0.5$ cm^{-1} for the limit, corresponding to a dissociation energy of $D_0(H_2) = 36\,118.6 \pm 0.5$ cm^{-1}. Recently, McCormack and Eyler [5] reinvestigated the spectrum of molecular lines using high-resolution, double-resonance laser techniques, and observed a complex structure of lines which differed from the predicted spectrum near the second dissociation limit. These authors concluded that a better theoretical understanding of the perturbed spectrum is necessary for a precise determination of the limit from the extrapolation of energies of high vibrational levels. During these experiments, McCormack and Eyler also observed the onset of the second dissociation continuum at $118\,377.2 \pm 0.20$ cm^{-1}, and reported a value of $D_0(H_2) = 36\,118.26 \pm 0.20$ cm^{-1}. In the present paper, we report on the measurement of the threshold of the second dissociation continuum, obtained by single-photon fluorescence-excitation spectroscopy near 84.5 nm. This has resulted in a precision of 0.08 cm^{-1} for the dissociation energy of the ground state of H_2.

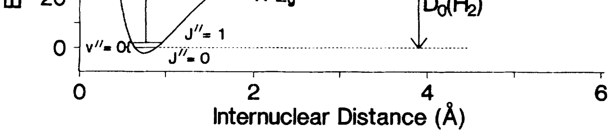

FIG. 1. Energy-level diagram showing the ground $X({}^1\Sigma_g^+)$ and excited states $B({}^1\Sigma_u^+)$ and $B'({}^1\Sigma_u^+)$ involved in the photodissociation of H_2, and used to determine the dissociation energy $D_0(H_2)$ of the ground state.

The experimental arrangement for generating coherent, tunable radiation in the region of 84.5 nm was essentially the same as that shown in Figs. 2 and 3 of Ref. [6], except that here the nonlinear medium was a pulsed jet of Kr gas. The primary source was a XeCl excimer laser (Lumonics TE-861M-2), operated at 50 mJ/pulse to optically pump two dye lasers and associated amplifier systems. One was transversely pumped to generate radiation at ~424 nm with a bandwidth of 0.2 cm^{-1}. This radiation was amplified and frequency doubled in a β-barium-borate crystal (CSK Co., Ltd.) to provide a beam (of ~15 kW peak power) at frequency ν_1, where $2\nu_1$ is resonant with the level $4p^5 5p[0, \frac{1}{2}]_0$ of Kr. The second was a single-longitudinal-mode (SLM) dye laser (modified Lumonics HyperDYE-SLM) used to generate radiation at ν_2, of output ~55 kW after amplification, with a bandwidth of 0.02 cm^{-1}, and tunable in the region of 414 nm. The two beams were synchronized and spatially overlapped, then focused with a lens (focal length of 25 cm) just below the nozzle of a pulsed jet (Laser Technics, LPV) of Kr gas, to generate tunable extreme ultraviolet (XUV) radiation at $\nu_{\rm XUV} = 2\nu_1 + \nu_2$, in pulses of ~4 ns duration. This radiation was incident (at right angles) on a nearby vertical beam of H_2 gas, in the region of supersonic expansion, ~50 mm below the 1-mm-diam nozzle of a second jet. A solar-blind photomultiplier (EMR 541G-08-17) and a concave mirror of 50 mm diameter and 76 mm radius of curvature were positioned on the mutually perpendicular axis and on opposite sides of the interaction region. The purpose of the mirror was to select a small region of ~1.2 mm diameter of the excited H_2 beam and to form an image of this region on the photomultiplier, thus limiting the detection to molecules in a small range of horizontal velocities. During this investigation, part of the beam of frequency ν_2 was used to irradiate a uranium hollow-cathode lamp for frequency calibration using the optogalvanic effect, and some was directed to a Fabry-Pérot etalon (with 1 cm^{-1} free spectral range) to ensure that this radiation remained in a single mode as its frequency was scanned. The signals from the photomultiplier, U lamp, and etalon were all sampled simultaneously by gated integrators and recorded digitally with a computer interface (Stanford Research Systems SR250 and SR245). While scanning the fluorescence-excitation spectra, the SLM beam was blocked every second pulse, to permit background subtraction. All spectra were scanned 10 to 15 times, then averaged by overlapping to within ±0.01 cm^{-1}, and digitally smoothed with a Gaussian filter of ~0.04 cm^{-1} bandwidth.

In preliminary experiments, both absorption and fluorescence-excitation spectra were recorded as the XUV radiation was scanned through the higher vibrational levels of the B and B' states (Fig. 1) and into the second dissociation continuum. For these experiments, the XUV radiation was incident on the H_2 beam only a few millimeters from the nozzle. Both spectra revealed intense molecular lines which completely obscured the threshold of the continuum. In order to obtain an unobstructed view of the threshold region, the fluorescence-excitation spectrum was investigated with delayed detection of fluorescence radiation at the Lyman-α line. For this purpose, the metastable $H(2s)$ atoms formed in the photodissociation process were detected by quenching with an electric field of ~150 V/cm, which coupled the $2s$ and $2p$ levels, resulting in the emission of Lyman-α radiation. The field was switched on ~200 ns after the excitation pulse, a delay sufficient to allow molecules in the B and B' states, and any $H(2p)$ atoms, to decay by radiation, long before the $2s$ atoms were quenched. Thus, it was possible to observe the threshold of the second dissociation limit clearly, and to measure its frequency directly by monitoring the onset of delayed fluorescence (synchronous with the quenching field) as the XUV radiation was slowly scanned in frequency.

Examples of observed spectra are shown in Fig. 2. In Fig. 2(a), the fluorescence was detected immediately following the excitation pulses, and the duration of sampling was sufficiently long (~750 ns) that the molecular fluorescence for excitation below the limit and that arising from quenched $H(2s)$ above the limit were observed. It is evident that the threshold of the continuum is obscured by the molecular features. The effective resolution of ~0.2 cm^{-1} determined from the molecular linewidths (and indicative of the XUV bandwidth) was insufficient to reveal the dissociation threshold. For Fig. 2(b), only the delayed fluorescence was sampled. No molecular features are in evidence, and the onset of the dissociation continuum is clearly seen. The intensity contour of the continuum shows no gradual onset (within the present sensitivity) but begins with an abrupt rise and steep linear slope, reaching a maximum within 3 cm^{-1}, and decreasing asymptotically to approximately half the maximum intensity. While this observed envelope is in qualitative agreement with the expected contour [7], the indication of structure near the intensity maximum and the extent of the linear portion suggest that a detailed theoretical examination would be useful. Also, it should be noted that, in principle, two dissociation thresholds are possible (although not detected here), since the product $H(1s)$ may be in the $F = 0$ or 1 hyperfine levels which differ in energy [8] by 0.047 cm^{-1}.

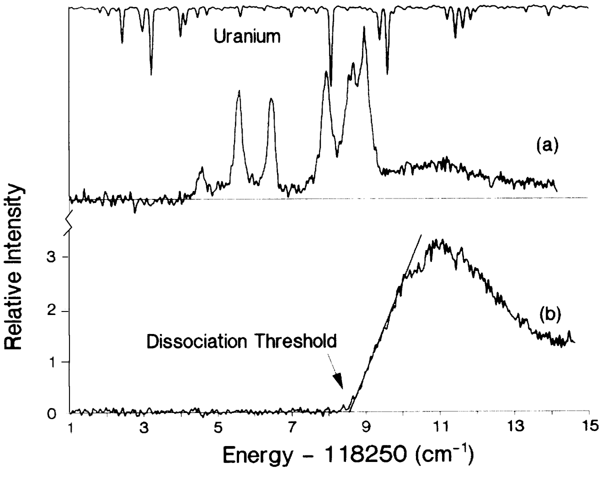

FIG. 2. Fluorescence-excitation spectra in the vicinity of the dissociation limit of ortho-H_2. (a) The spectrum obtained by sampling the fluorescence immediately after the laser excitation. (b) The spectrum of delayed fluorescence, arising from the quenching of atoms in the $2s$ state. The uppermost spectrum is the optogalvanic uranium spectrum used to calibrate ν_2.

For the present purpose of determining experimentally the dissociation threshold, a straight line was drawn through the linear portion of the onset using least squares, and extrapolated as shown in Fig. 2(b). Measurements from two spectra, each the average of twelve scans, yielded a value of 118 258.57 ± 0.04 cm^{-1}, for the dissociation threshold measured from $J''=1$, $v''=0$ of the ground state. To this value was added the rotational spacing [9] of 118.49 cm^{-1} between $J''=0$ and $J''=1$, to give the second dissociation limit of 118 377.06 cm^{-1}. On subtracting the 2*s*-1*s* separation [8] of 82 258.95 cm^{-1} we obtain $D_0(\mathrm{H}_2)=36\,118.11\pm0.064$ cm^{-1}, which includes an uncertainty of 0.024 cm^{-1}, arising from the hyperfine splitting of the H(1*s*) state mentioned above. Knowledge of the absolute accuracy requires an absolute frequency calibration of $\nu_{\mathrm{XUV}}=2\nu_1+\nu_2$, as well as an estimate of any Doppler shift arising from a horizontal velocity of the H_2 beam in the small portion of the interaction region being surveyed. The calibration of ν_{XUV} is, of course, dependent on the calibration of the dye-laser frequencies. The frequency ν_2 was calibrated during each scan to an accuracy of ±0.01 cm^{-1}, from the known U spectrum [10], recorded simultaneously with the fluorescence-excitation spectrum. (For all calibrations, the U atlas was corrected for the small systematic shift of +0.0011 cm^{-1}, determined by Sansonetti and Weber [11].) The two-photon resonance in Kr was determined in a separate experiment by using the tunable SLM dye laser with its frequency doubled through the barium-borate crystal to generate the third-harmonic radiation, with the resonance serving to enhance the output. The intensity was monitored by an electron multiplier (ITT F4074) at the exit slit of a 1-m spectrometer (MacPherson 225), and the intensity maximum was again calibrated with the U spectrum. The dye-laser frequency was doubled to give ν_1 (at ~15 kW peak power), and doubled again to $2\nu_1$, yielding a frequency of 94093.00 ± 0.04 cm^{-1} for the Kr level $5p[0,\frac{1}{2}]_0$ (in agreement with, but more precise than, an earlier value [12] of 94092.924 ± 0.15 cm^{-1}). Thus, ν_{XUV} could be determined to within ±0.04 cm^{-1} during a scan of the second dissociation limit. In estimating the possible uncertainty caused by a Doppler shift, the main contribution was found to arise from the inability to measure angles to better than $\Delta\theta=1.8°$, and resulted in an uncertainty, $\nu_0(v/c)\Delta\theta$, of 0.03 cm^{-1} (with the molecular velocity $v\sim2.4\times10^5$ cm/s, obtained from Doppler shifts of the molecular lines for known small-angle offsets of the H_2 beam from the vertical). When the above absolute uncertainties are combined in quadrature, the result is an absolute frequency precision of ±0.08 cm^{-1}, yielding

$$D_0(\mathrm{H}_2)=36\,118.11\pm0.08\ \mathrm{cm}^{-1}.$$

In similar experiments, the spectrum near the corresponding dissociation limit of para-H_2, shown in Fig. 3, was recorded. This region is ~118.5 cm^{-1} above the ortho-H_2 limit, and consequently the para-H_2 continuum is superimposed on that of ortho-H_2. Para-H_2 is the less abundant component of normal H_2, and therefore the para-H_2 spectrum has a lower signal-to-noise ratio than that of Fig. 2. The onset of the dissociation continuum is essentially clear, although broad structure caused by molecular absorption is evident just below the limit. Extrapolation of the linear onset leads to a preliminary value of 118 377.0 cm^{-1} for the second dissociation limit, in agreement with the value determined from the ortho-H_2 spectrum. However, further experimental refinement is necessary to establish the possible effect of the nearby absorption on the precision of the para-H_2 limit.

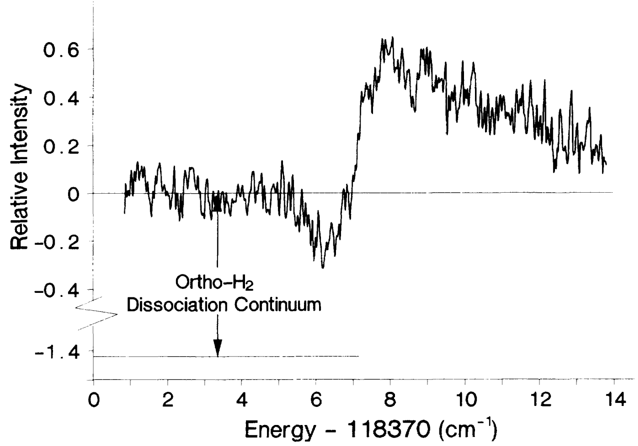

FIG. 3. Fluorescence-excitation spectrum near the dissociation limit of para-H_2 obtained by sampling the delayed fluorescence.

The present value for the dissociation energy of H_2 is compared with preceding experimental determinations and with the latest theoretical calculation in Table I. While the experimental values are in general agreement within the quoted accuracies, the precision of the present value gives credence to the theoretical calculations [1] of the dissociation energy together with the nonadiabatic, relativistic, and radiative corrections. Further improvements in experimental precision would be important, and are being pursued. Meanwhile, corresponding investigations with D_2 and HD are warranted.

Finally, it is noted that the present value of $D_0(\mathrm{H}_2)$ can be combined with experimental values of the ionization potentials of H and H_2 to provide an (experimental)

TABLE I. Summary of values of $D_0(\mathrm{H}_2)$.

	Reference	$D_0(\mathrm{H}_2)$ (cm^{-1})
Experiment	[3]	36 118.3
	[4]	36 118.6 ± 0.5
	[5]	36 118.26 ± 0.20
	Present	36 118.11 ± 0.08
Theory	[1,2]	36 118.09 ± 0.10

value for the dissociation energy of H_2^+, namely, $D_0(H_2^+) = D_0(H_2) + IP(H) - IP(H_2)$. For IP(H), we use the value [10] 109678.764 ± 0.01 cm^{-1}, and for $IP(H_2)$ an average of the recent determinations [13,14], $IP(H_2) = 124417.501 \pm 0.017$ and 124417.524 ± 0.015 cm^{-1}. These yield $D_0(H_2^+) = 21\,379.36 \pm 0.08$ cm^{-1}, which is in good agreement with the theoretical value [15,16] of 21 379.348 cm^{-1}.

This research was supported by the Natural Sciences and Engineering Research Council (NSERC), the Premier's Council Technology Fund, and the University of Toronto. A.B. is grateful to the University of Toronto and NSERC for scholarships during the course of this research. V.S. is thankful to the Ministère des Affaires Etrangères (France) and the National Research Council (Canada) for France-Canada fellowships. We are indebted to G. Herzberg and E. E. Eyler for helpful discussions on this problem.

---

[a] Visiting Scientist for several periods during the course of this research, on a France-Canada Exchange Programme. Permanent address: Université de Rennes I, Département de Physique Atomique et Moléculaire, Campus de Beaulieu, 35042 Rennes CEDEX, France.

[1] W. Kolos, K. Szalewicz, and H. J. Monkhorst, J. Chem. Phys. **84**, 3278 (1986), and references therein.

[2] K. Dressler and L. Wolniewicz, J. Chem. Phys. **85**, 2821 (1986).

[3] G. Herzberg, J. Mol. Spectrosc. **33**, 147 (1970).

[4] W. C. Stwalley, Chem. Phys. Lett. **6**, 241 (1970).

[5] E. F. McCormack and E. E. Eyler, Phys. Rev. Lett. **66**, 1042 (1991); E. F. McCormack, Ph.D. thesis, Yale University, 1989 (unpublished).

[6] P. R. Herman, P. E. LaRocque, R. H. Lipson, W. Jamroz, and B. P. Stoicheff, Can. J. Phys. **63**, 1581 (1985).

[7] C. W. Zucker and E. E. Eyler, J. Chem. Phys. **85**, 7100 (1986); A. C. Allison and A. Dalgarno, J. Chem. Phys. **55**, 4342 (1971).

[8] S. Bashkin and J. O. Stoner, Jr., *Atomic Energy Levels and Grotrian Diagrams* (American Elsevier, New York, 1975), Vol. 1.

[9] J. V. Foltz, D. H. Rank, and T. A. Wiggins, J. Mol. Spectrosc. **21**, 203 (1966).

[10] B. A. Palmer, R. A. Keller, and R. Engleman, Los Alamos Scientific Laboratory Report No. LA-8251-MS, UC 34a, 1980 (unpublished).

[11] C. J. Sansonetti and K.-H. Weber, J. Opt. Soc. Am. B **1**, 361 (1984).

[12] V. Kaufman and C. J. Humphreys, J. Opt. Soc. Am. **59**, 1614 (1969).

[13] Ch. Jungen, I. Dabrowski, G. Herzberg, and M. Vervloet, J. Chem. Phys. **93**, 2289 (1990).

[14] E. McCormack, J. Gilligan, C. Cornaggia, and E. E. Eyler, Phys. Rev. A **39**, 2260 (1989).

[15] L. Wolniewicz and J. D. Poll, Mol. Phys. **59**, 953 (1986); and erratum, **66**, 701(E) (1989).

[16] L. Wolniewicz and T. Orlikowski, Mol. Phys. **74**, 103 (1991).